arXiv:cond-mat/9908168v3 [cond-mat.dis-nn] 10 Nov 2000

Impurity-induced polaritons in a one-dimensional chain*

A. Yamilov,† L.I. Deych‡ and A.A. Lisyansky†
†*Department of Physics, Queens College of CUNY, Flushing, NY 11367*
‡*Department of Physics, Seton Hall University, 400 South Orange Ave, South Orange, NJ 07079*
(February 1, 2008)

A detailed analytical study of an impurity induced polariton band arising inside a spectral gap between lower and upper polariton branches is presented. Using the microcanonical method, we calculate the density of states and localization length of the impurity polaritons. Analytical results are compared with numerical simulations and excellent agreement is found.

I. INTRODUCTION

An opportunity to create Anderson localized states of electromagnetic excitations in disordered dielectrics has attracted a great deal of attention during the last two decades.[1,2] Though the localization of light in three-dimensional uniform-on-average random systems proved to be difficult to achieve, new opportunities opened up with development of the structures with periodically modulated dielectric properties, so called photonic crystals.[3,4] It was first suggested in Ref. 5 that the photon localization can be more easily achieved if the photon density of states (DOS) is depleted at certain frequency domains. Photonic crystals allow the creation of photon band-gaps, regions of frequencies where the photon DOS is zero. Introducing isolated defects in such structures, one can create local photon modes similar to well known defect phonon modes in regular crystals[6–10] or electron impurity states in semiconductors.[11] A forbidden gap in the photonic spectrum occurs when the electromagnetic wave length becomes comparable to the lattice constant. Consequently, for microwave, infrared and visible ranges, the photonic crystal is a structure of macroscopic dimensions. Local states in these structures also arise due to defects of macroscopical dimensions. The great interest in photonic crystals is promoted by their highly unusual quantum electrodynamic properties. For instance, spontaneous emission, which is completely suppressed within the frequency range of the band gaps,[12] can be effectively controlled by introducing local modes.[13,14]

The intriguing possibilities of photonic crystals initiated interest in optical effects in other types of photonic band-gaps. Such gaps can arise, for example, between different polariton branches. The fact that the frequency region between polariton branches can represent a stop-band for electromagnetic waves propagating in certain directions has been well known for a long time. The reflection coefficient in this situation can reach the magnitude of 90 percent or even greater. This effect was used in the 40's and 50's in order to create monochromatic infrared beams (it was called the method of residual or reststrahlen rays, and the respective spectral interval was called the reststrahlen region). In certain cases, however, the stop bands exist for all the directions, and then a genuine spectral gap arises with the same consequences for quantum electrodynamics as in the case of photonic crystals. This was first realized in Ref. 15, where it was shown that a two-level atom can form an atom-field coupled states with suppressed emission similar to the states discussed in Ref. 16 for photonic crystals. Periodic arrangement of such two-level systems produces an impurity-induced polariton band within the polariton gap.[17]

Local polariton states associated with a regular isotopic defect without any intrinsic optical activity were introduced in Refs. 18,19. These states are coupled states of electromagnetic excitations with phonons (or excitons), with both components, including the electromagnetic component, being localized in the vicinity of the defect. These states are, in a certain sense, analogous to local photons in photonic crystals considered in Refs. 13,14, although they arise due to microscopic impurities in regular crystal lattices. On the other hand, local polaritons can be considered as local excitations of a crystal coupled with the electromagnetic field. Regular local phonons (excitons) also interact with the electromagnetic field, but this interaction results mainly in absorption of light and radiative decay of the states.[10] The local polaritons arise in the region where electromagnetic waves do not propagate, and there are, therefore, neither defect induced absorption of light nor radiative damping of the local states. The electromagnetic interaction leads in this case to new optical effects, and strongly affects the properties of the local states. It is well known, for instance, that local phonons or excitons in a 3D system (as well as local photons in photonic crystals) arise only

*J. Opt. Soc. Amer. B, 2000, 17, No. 9, 1498-1508.

if the "strength" of a defect exceeds a certain threshold. Local polaritons in systems with an isotropic dispersion split off the allowed band without a threshold even in three dimensions.[18] This effect is caused by the interaction with electromagnetic field, which results in the Van-Hove singularity in the polariton DOS.

One of the optical effects caused by local polaritons is resonant tunneling of electromagnetic wave with gap frequencies. This effect was first suggested in Ref. 20, where the results of numerical simulation of electromagnetic wave propagation through a relatively short 1D chain with a single defect were reported. It was found that the transmission coefficient at the frequency of the local polariton state increases dramatically up to the a value close to unity. In spite of the general understanding that local states should produce local tunneling, this result still seems surprising because transmission of light is effected by a defect with microscopic dimensions much smaller than the light's wavelength. In addition, the energy of the electromagnetic component of local polaritons is much smaller than that of the phonon component. Traditional wisdom based upon properties of conventional propagating polaritons tells that, in such a situation, most of the incident radiation must be simply reflected. The results of Ref. 20 demonstrated that this logic does not apply to local polaritons. The physical explanation of the result can be given on the basis of consideration of local polaritons as the result of interaction between electromagnetic field and local phonons. The latter have macroscopic dimensions comparable with light's wavelength, making the interaction effective. An electromagnetic wave is carried through a sample by phonons, which is tunneling resonantly due to the local state with mostly phonon contribution. Tunneling was confirmed in Refs. 21,22, where we analytically calculated the transmission coefficient through a linear chain with a single defect. We found that a light impurity indeed gives rise to the resonance transmission through the forbidden gap of the polariton spectrum. The resonance occurs when the defect is placed at the center of the chain. The transmission at the resonance becomes independent of the chain's length and reaches the value of unity if the resonance frequency coincides with the center of the polariton gap. The analytical calculations provided an explanation for the numerical results of Ref. 20, in particular it explained a strongly asymmetrical frequency profile of the transmission coefficient, and the presence of a deep minimum following directly after the maximum.

Analytical calculations in Ref. 22 were supplemented with numerical simulations of the electromagnetic wave transmission through the chain with a finite concentration of impurities. The simulations demonstrated the development of a defect-induced polariton band within the forbidden polariton gap. In this paper, we present results of an analytical study of properties of this band. Neglecting spatial dispersion of phonons, we are able to obtain analytical expressions for DOS and the Lyapunov exponent for the band in the limit of large concentration of impurities $l_0/l_{def} \gg 1$, where l_{def} is the average distance between impurities, and l_0 is the localization length of the single local polariton state. In this limit the method of microcanonical ensemble, complemented by expansion over $(l_0/l_{def})^{-1}$, gives the DOS of an effective system with a uniform distribution of impurities, and describes its renormalization caused by local fluctuations of impurity positions. It also reveals localization of the states of the band, which are all localized due to the one-dimensional nature of the model. The properties of this polariton band are found to be drastically different from that of the band produced by two-level atoms.[17] The analytical results show excellent agreement with numerical calculations and lead to suggestions regarding experimental observation of the impurity induced polariton bands.

II. THE MODEL OF ONE-DIMENSIONAL POLARITONS AND THE METHOD OF CALCULATIONS

1. The model

The main objective of the present paper is to study properties of the impurity induced polariton band arising within the polariton gap of a one dimensional chain of atoms with dipole moments P_n, where n refers to a position of an atom in the chain. Dynamics of the chain interacting with a scalar "electromagnetic field" $E(x)$ is described within the tight-binding approximation with an interaction between nearest neighbors only,

$$(\Omega_n^2 - \omega^2)P_n + \Phi(P_{n+1} + P_{n-1}) = \alpha E(x_n), \qquad (1)$$

where Φ is the parameter of the interaction between the dipoles, α is a coupling parameter between the dipoles and the electromagnetic field, and Ω_n^2 represents a site energy. We shall assume that the chain is composed of atoms of two different types, which differ in their site energy only. In this case Ω_n^2 can be presented in the following form:

$$\Omega_n^2 = \Omega_0^2 + \Delta\Omega^2 c_n, \qquad (2)$$

where $\Delta\Omega^2 = \Omega_1^2 - \Omega_0^2$, Ω_0^2 and Ω_1^2 are site energies of the respective atoms, and c_n is a random variable which takes values 0 and 1 with probabilities $1-p$ and p, respectively. We assume that $p \ll 1$ so that Ω_0 is attributed to host atoms, whereas Ω_1 corresponds to the impurities. Eq. (1) can be interpreted in terms of both exciton-like and phonon-like excitations. In the latter case, $\Delta\Omega^2 = (1-M_{imp}/M_{host})\omega^2$, where M_{host} and M_{imp} are the masses of host atoms and impurities, respectively.

Polaritons in the system arise as collective excitations of dipoles (polarization waves) coupled to the scalar electromagnetic wave, $E(x_n)$. The equation of motion of the electromagnetic component is given by the Maxwell equation:

$$\frac{\omega^2}{c^2}E(x)+\frac{d^2E}{dx^2}=-4\pi\frac{\omega^2}{c^2}\sum_n P_n\delta(na-x), \qquad (3)$$

where c is the speed of the electromagnetic wave in vacuum and a is the distance between two nearest-neighbor dipoles. Eqs. (1) and (3) present a *microscopic* description of the transverse electromagnetic waves propagating along the chain in the sense that it does not make use of the concept of the dielectric permeability, and takes into account all modes of the field including those with wave numbers outside of the first Brillouin band.

Considering propagation of the electromagnetic wave as a sequence of scattering events separated by free propagation, one can present Eq. (3) in a discrete form. The entire system of dynamic equations (1) and (3) can then be transformed into a transfer-matrix form:

$$v_{n+1}=\hat{\tau}_n v_n, \qquad (4)$$

Vectors v_n with components $(P_n, P_{n+1}, E_n, E'_n/k)$, where E_n and E'_n are electromagnetic field and its derivative at the n-th site, represent the state of the system. In general, the matrix $\hat{\tau}_n$, which describes the field propagation between adjacent sites, is a 4×4 matrix.[20–22] This makes an analytical consideration of Eq. (4) very cumbersome, even in the case of a single impurity. At the same time, numerical simulations carried out in Refs. 21,22 showed that most of the features of the impurity induced polariton band are well reproduced even when the interaction between the dipoles (spatial dispersion) is neglected. In this approximation, the two first components of the dynamic vector v_n are easily expressed in terms of the other two, and the transfer matrix $\hat{\tau}_n$ becomes a 2×2 matrix of the following form:

$$\hat{\tau}_n=\begin{pmatrix}\cos ka & \sin ka\\ -\sin ka+\beta_n(ka)\cos ka & \cos ka+\beta_n(ka)\sin ka\end{pmatrix}. \qquad (5)$$

The parameter β_n

$$\beta_n=\frac{d^2}{\omega^2-\Omega_n^2}; \qquad (6)$$

with $d^2=4\pi\alpha/a$ represents the polarizability of the n-th dipole.

The main object of interest in studies of one-dimensional disordered systems is the Lyapunov exponent (LE), λ, which in our case can be defined as[23]

$$\lambda=\lim_{L\to\infty}\frac{1}{L}\ln\frac{\left\|\prod_1^N\hat{\tau}_n v_0\right\|}{\|v_0\|}, \qquad (7)$$

where L is the total length of the chain consisting of N atoms. It is well-known that the quantity defined by Eq. (7) is non-random (self-averages). It characterizes the spatial extent of the envelope of system eigenstates, all of which are localized in one dimension (see Ref. 25 and references therein). The same quantity also describes the typical value of the transmission coefficient, T, of an external excitation incident upon the system: $T_{typ}\simeq\exp(-\lambda L)$, and through the Thouless relation[24] it determines the DOS of the system. Calculation of LE in the spectral region of the polariton gap of the pure system is the main task of this section.

2. The Method of Microcanonical Ensemble

The major problem with calculating of LE or DOS in the region of impurity bands is that a simple concentration expansion is not able to describe the impurity band. Electron and phonon impurity bands have been intensively studied in the past (see, for example, Ref. 25). In the limit of extremely small concentration of impurities, $(pl_0)/a\ll1$, it was proved possible to provide a regular systematic of the arising states and use statistical arguments to describe their DOS.[6] Another method used for this type of calculations employed the so-called phase formalism (see Ref. 25 and references therein). This approach allowed one to calculate DOS of impurity bands in different spectral regions, including exponential behavior at the tails of the band for both small and large, $(pl_0)/a\gg1$, concentrations. In the case of local polaritons the localization length, l_0, of an individual local state can be so large that one has to deal with the situation described by the latter inequality even in the case of a rather small concentration of impurities. Therefore, in this paper we focus mainly upon the properties of the well-developed polariton impurity band when individual local states are overlapped. To this end we use the method of the microcanonical ensemble, which was first suggested for analytical calculations of LE in a one-dimensional single-band model of a disordered alloy.[23] The advantage of this method over other methods of DOS calculations is that it allows one to calculate simultaneously both DOS and the localization length. Its main shortcoming is that, as we shall see later, this method is a version of "effective media" methods, and as such it is unable to describe DOS near fluctuation boundaries of the spectrum. At the same time the results obtained allow a clear physical interpretation and, as follows from comparison with numerical simulations, they quite accurately describe properties of the bulk of the impurity band.

The starting point of our calculations is the general definition of LE given by Eq. (7). In spite of LE being a self-averaging quantity, it is convenient in practical calculations to perform averaging over the random configurations of the impurities. The regular ensemble of the realization is described by the fixed concentration of the impurities p, while their total number can vary from realization to realization. Therefore one can distinguish two causes for fluctuations: (1) local arrangements of the impurities and (2) the total number of the impu-

rities. The main idea of the method of microcanonical ensemble is to reduce the finite size fluctuations in the system, eliminating the fluctuations of the total number of impurities. Such an ensemble with a fixed number of impurities is called the microcanonical ensemble in analogy with statistical physics. At the same time the result of the averaging in the limit $L \to \infty$ should not depend upon the type of ensemble used by virtue of the self-averaging nature of LE. The key idea of the microcanonical method is based on the assumption that with one cause of fluctuations eliminated, one can obtain reliable results when the microcanonical ensemble average of $\langle \ln(...) \rangle$ is replaced by $\ln\langle ... \rangle$. Such a substitution gives an exact result in the case of commutating matrices, and leads to an excellent agreement between analytical calculations and simulations in the case of 2×2 matrices with a single band spectrum.[23]

Using the microcanonical ensemble, one can evaluate the average over all matrix sequences using the following expression derived in Ref. 23:

$$\left\langle \prod_1^N \hat{\tau}_n \right\rangle = \binom{N}{pN}^{-1} \frac{1}{(pN)!} \frac{\partial^{pN}}{\partial x^{pN}} \left(\hat{\tau}_0 + x\hat{\tau}_1\right)^N \Big|_{x=0}, \tag{8}$$

where $\hat{\tau}_0$ and $\hat{\tau}_1$ are host and defect matrices, respectively and x is a free parameter. The derivative in Eq. (8) then can be presented in the form of the Cauchy integral

$$\left\langle \prod_1^N \hat{\tau}_n \right\rangle = \binom{N}{pN}^{-1} \frac{1}{2\pi i} \int_C dx \frac{\nu^N(x)}{x^{pN+1}} \hat{D}(x), \tag{9}$$

where the contour of integration C is taken on the complex plane around $x = 0$, $\nu(x)$ is the largest eigenvalue of the matrix $\hat{\tau}_0 + x\hat{\tau}_1$, and the matrix $\hat{D}(x)$,

$$\hat{D}(x) = \nu^{-N}(x) \left(\hat{\tau}_0 + x\hat{\tau}_1\right)^N, \tag{10}$$

has eigenvalues not exceeding 1 in absolute value. In the limit of large N the above integral can be evaluated by the saddle point method. As the result we arrive at the following expression for the complex valued LE, $\widetilde{\lambda}$:

$$\begin{aligned} \widetilde{\lambda} &= \lim_{N\to\infty} \frac{1}{L} \ln \left[\text{largest eigenvalue } \left\langle \prod_1^N \hat{\tau}_n \right\rangle \right] \\ &= \frac{1}{a} \left[\ln \nu(x_0) - (1-p) \ln \frac{x_0}{1-p} + p \ln p \right], \end{aligned} \tag{11}$$

where x_0 is defined by the saddle point equation

$$\frac{\partial \ln \nu(x)}{\partial \ln x}\Big|_{x=x_0} = p. \tag{12}$$

The real part of $\widetilde{\lambda}$ given by Eq. (11) represents LE, while its imaginary part according to Thouless[24] gives the integral density of states $N(\omega)$ in the impure system:

$$\lambda = \mathrm{Re}\left[\widetilde{\lambda}\right], \tag{13}$$

$$N(\omega) = -\frac{1}{\pi} \mathrm{Im}\left[\widetilde{\lambda}\right]. \tag{14}$$

The eigenvalues of the matrix $\hat{\tau}_0 + x\hat{\tau}_1$ can be found from the equation

$$\frac{\nu}{1+x} + \frac{1+x}{\nu} = \kappa(x) = 2\cos(ka) + \frac{\beta_0 + x\beta_1}{1+x}, \tag{15}$$

where β_0 and β_1 are polarizabilities of the host and defect atoms, respectively.

It is convenient to rewrite Eqs. (11) and (15) in terms of a new variable $y = x/(1+x)$:

$$\kappa(y) = (1-y)\nu(y) + \frac{1}{(1-y)\nu(y)} = \kappa_0(\omega) + yF(\omega), \tag{16}$$

$$\kappa_0(\omega) = 2\cos(ka) + d^2 ka \sin(ka) \frac{1}{\omega^2 - \Omega_0^2}, \tag{17}$$

$$F(\omega) = d^2 ka \sin(ka) \frac{\Omega_1^2 - \Omega_0^2}{(\omega^2 - \Omega_0^2)(\omega^2 - \Omega_1^2)}. \tag{18}$$

In the long-wave limit $\epsilon = ka \ll 1$ functions $F(\omega)$ and $\kappa_0(\omega)$ can be simplified and presented in the form, which clarifies their physical meaning:

$$\begin{aligned} F(\omega) &\simeq \epsilon^2 f(\omega), \\ \kappa_0(\omega) &\simeq 2 + \epsilon^2 \gamma(\omega), \end{aligned}$$

where $f(\omega)$ is defined according to

$$f(\omega) \simeq \frac{d^2(\Omega_1^2 - \Omega_0^2)}{(\omega^2 - \Omega_0^2)(\omega^2 - \Omega_1^2)} \tag{19}$$

and represents the difference $\beta_1 - \beta_0$ between polarizabilities (6) of the impurities and host atoms. Function $\gamma(\omega)$ defined as

$$\gamma(\omega) = 1 + \frac{d^2}{\Omega_0^2 - \omega^2} \tag{20}$$

is the longwave dielectric function of the pure chain.

Similarly, Eq. (11) transforms into

$$\begin{aligned} \widetilde{\lambda}(p) &= \ln\left[(1 - y_0(p))\nu(y_0(p))\right] \\ &\quad - \left[p \ln \frac{y_0(p)}{p} + (1-p) \ln \frac{1 - y_0(p)}{1-p} \right], \end{aligned} \tag{21}$$

with the saddle point equation reading as

$$\pm \frac{y(1-y)F}{\sqrt{(\kappa_0 + yF)^2 - 4}} + y \Big|_{y=y_0} = p, \tag{22}$$

The choice of the sign in Eq. (22) is determined by the requirement to use the greatest of the eigenvalues ν. Introduction of the new variable y turns $\kappa(y)$ in a linear function of y essentially simplifying future calculations.

III. THE LYAPUNOV EXPONENT AND THE DENSITY OF STATES

3. Boundaries of the impurity band

Dielectric function $\gamma(\omega)$ determines the frequency region of the polariton gap: for $\Omega_0^2 < \omega^2 < \Omega_0^2 + d^2$ it is negative, and hence, propagating modes do not exist in this region. We shall assume that the defect frequency Ω_1^2 obeys the inequality $\Omega_0^2 < \Omega_1^2 < \Omega_0^2 + d^2$, so that the impurity induced band develops inside the gap of the original spectrum. As we already mentioned, the approach we use in the paper belongs to the class of effective-medium approximations since we neglect here certain kinds of fluctuations in the system. It is natural to expect, therefore, that within this approach the impurity band would have well-defined spectral boundaries outside of which the differential DOS remains exact zero. Our first goal is to determine these boundaries and find the concentration dependence of the width of the impurity band. The differential DOS, $\rho(\omega) = dN(\omega)/d\omega$, takes on non-zero values when $\widetilde{\lambda}(\omega)$ acquires a non-constant imaginary part. Rewriting Eq. (21) in the form

$$\widetilde{\lambda}(\omega) = \frac{1}{a}\ln\left[\frac{1}{2}\left(\kappa_0 + y_0 F \pm \frac{y_0(1-y_0)F}{p-y_0}\right)\right] - \frac{1}{a}\left[p\ln\frac{y_0}{p} + (1-p)\ln\frac{1-y_0}{1-p}\right], \quad (23)$$

one can see that in the case of real y_0, $\mathrm{Im}\,\widetilde{\lambda}(\omega)$ can be either zero or π (the latter happens when the argument of ln is negative). In both cases differential DOS is obviously zero, and it can only take on a non-zero value when y_0 becomes complex. Eq. (22), which defines y_0, is formed by a polynomial of the third order with real coefficients; therefore it has either three real roots or one real solution and a complex conjugated pair. In order to describe formation of the polariton band, one has to select the root, which has a complex component in a certain frequency interval and yields positive LE. Comparison with numerical simulations shows that the choice of only one of three saddle point, according to above mentioned criteria, produces the correct description of the impurity band. It is not difficult to show that at the frequency where $y_0(\omega)$ becomes complex, the derivative $\partial y_0/\partial\omega$ diverges. This fact gives us an explicit equation for the spectrum boundaries. From Eq. (22) one can find that the divergence occurs when y_0 satisfies the equation

$$y_0^3 F\left[F(1-p)+\kappa_0\right] + y_0^2\left[\kappa_0 F(1-3p) + k_0^2 - 4\right] + y_0\kappa_0\left(F - 2\kappa_0^2 + 4\right) + p(\kappa_0^2 - 4) = 0. \quad (24)$$

Eqs. (22) and (24) define the concentration dependence of the boundaries of the polariton impurity band. An approximate solution of this equation can be obtained as a formal series in powers of parameter $\epsilon = ka$. It will be seen, however, from the results that the actual expansion parameter in this case is $1/pl_0 \ll 1$. The solution of Eq. (22) with the accuracy to ϵ^2 can be obtained in the form:

$$y = p - p(1-p)\frac{f}{2\sqrt{pf-\gamma}}\epsilon + p(1-p)\frac{2(pf-\gamma)f(1-2p) - fp(1-p)}{8(pf-\gamma)^2}f^2\epsilon^2, \quad (25)$$

where $y = p$ is the only non-vanishing zero order approximation for y. Since two other solutions, $y = 0$, correspond to a singular point of the integral (9), the chosen solution $y = p$ represents the only saddle point accessible within our perturbation scheme. Using additional criteria outlined above we verify that the solution given by Eq. (25) correctly reproduces the behavior of LE. Substituting Eq. (25) into Eq. (21) one finds the complex LE in the long wavelength approximation:

$$\widetilde{\lambda}(\omega) = \frac{\omega}{c}\left(\sqrt{pf(\omega)-\gamma(\omega)} - \frac{p(1-p)f^2(\omega)}{8[pf(\omega)-\gamma(\omega)]}\epsilon\right). \quad (26)$$

According to Eq. (26), $\widetilde{\lambda}(\omega)$ acquires an imaginary part at frequencies obeying the inequality

$$pf(\omega) - \gamma(\omega) \le 0, \quad (27)$$

The boundaries are determined by the respective equation $pf(\omega) - \gamma(\omega) = 0$, which coincides with the long wavelength limit of Eq. (24). This equation determines two points where $pf(\omega) - \gamma(\omega)$ changes sign to negative:

$$\omega_{il,pu}^2 = \frac{1}{2}(\Omega_0^2 + \Omega_1^2 + d^2) \pm \frac{1}{2}\sqrt{(\Omega_0^2 + d^2 - \Omega_1^2)^2 + 4d^2(\Omega_1^2 - \Omega_0^2)p}, \quad (28)$$

The first of these solutions belongs to the initial polariton band-gap and as such represents the low-frequency boundary of the new impurity band. The second one lies outside of the gap and is a bottom frequency, modified by impurities, of the upper polariton branch of the initial spectrum. These two frequencies, however, are not the only points where the expression $pf(\omega) - \gamma(\omega)$ turns negative. Two other points are

$$\omega_{pl}^2 = \Omega_0^2, \qquad \omega_{iu}^2 = \Omega_1^2, \quad (29)$$

and the change of the sign at these points occurs through infinity of $pf(\omega) - \gamma(\omega)$ rather than through zero. These two frequencies do not depend upon the concentration of impurities and present, therefore, stable genuine boundaries of the spectrum. This property of Ω_0 and Ω_1 is due to their resonance nature (they correspond to the poles of the respective polarizabilities) and disappears when, for example, the spatial dispersion is taken into account. At the same time, the numerical simulations of Ref. 22, in which the spatial dispersion was taken into consideration, indicate that the shift of these frequency from their

initial values is negligibly small for realistic values of the inter-atom interaction parameter Φ, even for a relatively large concentration of impurities.

These four frequencies set the modified boundaries of the initial polariton spectrum of the pure system (ω_{pl}^2, ω_{pu}^2), and boundaries of the newly formed impurity band (ω_{iu}^2, ω_{il}^2). The lower boundary of the forbidden gap of the crystal, Ω_0, is not affected by the impurities - the singularity in the polariton DOS at this point survives for any concentrations of defects. The upper boundary of the band gap, ω_{pu}, shifts toward higher frequencies with the concentration and when $p = 1$, it coincides with the upper band boundary of the new crystal, $\Omega_L^i = \sqrt{\Omega_1^2 + d^2}$. Frequencies ω_{il} and ω_{iu} give approximate values for the lower and upper boundaries of the impurity induced pass band which arises inside the original forbidden gap $\Omega_0 < \omega_{il} < \omega_{iu} < \sqrt{\Omega_0^2 + d^2}$. The impurity band grows asymmetrically with concentration: while its lower boundary moves towards Ω_0 with an increase of the concentration, the upper edge remains fixed at $\omega_{iu} = \Omega_1$. Such a behavior of the impurity band agrees well with our numerical results.[22]

The width of the impurity induced band defined in terms of squared frequencies $\Delta_{im}^2 = \omega_{iu}^2 - \omega_{il}^2$ can be found from Eqs. (28) and (29) as

$$\Delta_{im}^2 = \frac{1}{2}\sqrt{(\Omega_0^2 + d^2 - \Omega_1^2)^2 + 4d^2(\Omega_1^2 - \Omega_0^2)p} - \frac{1}{2}(\Omega_0^2 + d^2 - \Omega_1^2). \tag{30}$$

For Ω_1 not very close to the upper boundary of the initial polariton gap, $\Omega_L = \sqrt{\Omega_0^2 + d^2}$, the linear in p approximation is sufficient to describe the concentration dependence of the band width

$$\Delta_{im}^2 \approx \frac{d^2(\Omega_1^2 - \Omega_0^2)p}{\Omega_0^2 + d^2 - \Omega_1^2}. \tag{31}$$

When Ω_1, however, happens to be close to Ω_L, a crossover is possible from the linear dependence (31) to the square root behavior:

$$\Delta_{im}^2 \approx \sqrt{d^2(\Omega_1^2 - \Omega_0^2)p}. \tag{32}$$

The condition for such crossover to occur is

$$1 \ll p \ll \frac{(\Omega_0^2 + d^2 - \Omega_1^2)^2}{4d^2(\Omega_1^2 - \Omega_0^2)}.$$

4. The Lyapunov exponent and the density of states far from the spectrum boundaries

Using Eqs. (13), (14) and (26) one can calculate LE and the integral DOS for different regions of the spectrum. For allowed bands, $(0, \Omega_0)$, (ω_{il}, Ω_1), (ω_{pu}, ∞), one has

$$\lambda(\omega) = -\frac{p(1-p)f^2}{8\,(pf-\gamma)}\frac{\omega}{c}\epsilon + O(\epsilon^2), \tag{33}$$
$$N(\omega) = \frac{1}{\pi}\frac{\omega}{c}\sqrt{|pf-\gamma|} + O(\epsilon^2);$$

for forbidden bands, $(\Omega_0, \omega_{il}), (\Omega_1, \omega_{pu})$, we obtain

$$\lambda(\omega) = \frac{\omega}{c}\left\{\sqrt{pf-\gamma} - \left[\frac{p(1-p)f^2}{8\,(pf-\gamma)}\right]\epsilon\right\}, \tag{34}$$
$$N(\omega) = 0.$$

One can see from Eqs. (33) and (34) that within allowed bands, DOS appears in the zero order of the formal expansion parameter ϵ, while LE starts from the first order. For the forbidden bands the situation is reversed: LE contains a term of zero order in ϵ, while DOS in this order disappears. This observation suggests a simple physical interpretation of the microcanonical approximation in conjunction with the expansion over ϵ. Analysis of the series in this parameter shows that the actual small parameter is $a/(pl_0) = l_{def}/l_0$, where l_{def} is a mean distance between impurities. The zero order expansion in this parameter can be interpreted as a uniform continuous ($l_{def} \to 0$) distribution of impurities with concentration p. The results in this approximation then corresponds to the polariton impurity band which would exist in such a uniform system. The parameter l_{def}/l_0 in this case is a measure of disorder in the distribution of impurities, which leads to the localization of excitations described by the DOS in Eq. (33) with the localization length, $l^{-1} = \lambda$, presented in the first line of the same equation.

Let us now consider frequencies in the interval $\omega \in (0, \Omega_0) \cup \left(\Omega_L^i, \infty\right)$, where pass bands of the pure chains composed of either host or impurity atoms overlap. The DOS in this region can be written in a physically transparent form

$$N(\omega) = \sqrt{(1-p)\,N_0^2(\omega) + pN_1^2(\omega)}; \tag{35}$$

where $N_0(\omega)$ and $N_1(\omega)$ are integral DOS in pure chains containing host atoms or impurities, respectively. In the remaining portion of the initial spectrum $\omega \in \left(\omega_{up}, \Omega_L^i\right)$ (but not very close to the boundary ω_{up}, where the expansion ceases to be valid) DOS can be presented as $N(\omega) = \sqrt{(1-p)\,N_0^2(\omega) - pl_1^2(\omega)}$, where l_1 is the penetration length through the polariton gap of the 100% impure chain.

Our main goal, however, is obtaining DOS and LE of the impurity induced band, $\omega \in (\omega_{il}, \Omega_1)$. Near the center of this region, the DOS can be presented in the following form

$$N\,(\omega) = \frac{1}{\pi l_0}\left[1 + \frac{4|\gamma|\omega_c}{pd^2}\,(\omega - \omega_c) + O\left(\left(\frac{\omega - \omega_c}{d}\right)^2\right)\right], \tag{36}$$

where ω_c is the center of the impurity band, which in the linear in p approximation is

$$\omega_c^2 = \Omega_1^2 - \frac{1}{2}\Delta_{im}^2, \tag{37}$$

where Δ_{im}^2 is the width of the band in terms of squared frequencies defined in Eq. (31). The first term in Eq. (36) represents the total number of states between ω_{il} and the center of the band; it is interesting to note that this number does not depend upon concentration of impurities. The coefficient at the second term gives the differential DOS at the center and can be rewritten as

$$\rho(\omega_c) = \frac{4\left|\gamma\right|\omega_c}{\pi l_0 p d^2} = \frac{2}{\pi l_0 \delta}, \tag{38}$$

where $\delta = \Delta_{im}^2/2\omega_c$ is an approximate expression for the impurity band width $\delta \simeq \Omega_1 - \omega_{il}$. This DOS has a simple meaning of the average density of states uniformly distributed through the entire band over the distance equal to $l_0/2$. In one dimensional uniform systems the wave number of the respective excitations, k, is simply connected to $N(\omega)$: $k = \pi N(\omega)$. The differential DOS would in this case be proportional to the inverse group velocity. Accordingly, $1/\pi\rho(\omega_c)$ given by Eq. (38) can also be viewed as a group velocity, v, of excitations in the center of our impurity band in the case of the uniform distribution of impurities. The expression for v can also be presented as

$$v = \frac{d^2}{4\omega_c^2\left|\gamma\right|^{3/2}} pc \ll c, \tag{39}$$

which demonstrates that polariton excitations of the impurity band have much slower velocities not only compared to c but also to the velocities at both regular polariton branches.

Expanding Eq. (33) for LE about the center of the band, we obtain a parabolic frequency dependence of the localization length of the impurity polaritons

$$l(\omega) = \lambda(\omega)^{-1} = 2l_0(pl_0)\left[1 - \frac{20\gamma^2}{p^2}\left(\frac{\omega^2-\omega_c^2}{d^2}\right)^2\right]. \tag{40}$$

One can see from this expression that $l(\omega)$ reaches its maximum value $2pl_0^2$ at the center of the band. It is important to note that the localization length here grows linearly with the concentration, whereas it is LE that grows with concentration for frequencies outside of the impurity band. An increase of the concentration of the impurities also results in fast ($\propto 1/p^2$) flattening of the maximum in the localization length, the fact we first noticed in our numerical simulations.[22]

The frequency dependence of LE, defined by Eqs. (21) and (22), is shown in Fig. 1. For frequencies corresponding to the impurity band, LE drops sharply (the localization length increases); it then diverges at the upper boundary of the impurity band. This divergence has the same origin as LE divergence at the lower boundary of the band gap of the original crystal, where due to the specificity of the polariton spectrum, the wave vector becomes infinite. The concentration dependence of LE and integral DOS for some frequency $\omega_0 \in (\Omega_0, \Omega_1)$ is shown in Fig. 2. For $p = 0$ this frequency belongs to the forbidden gap, thus DOS is zero. With an increase of the concentration LE decreases (the localization length increases). For the concentration when the lower boundary of the impurity band crosses ω_0, DOS becomes non-zero and in $\lambda(\omega)$ the crossover between behaviors described by Eqs. (34) and (33) occurs. In Fig. 3 we compare the results of our analytical calculations with numerical simulations of Ref. 22. The comparison shows an excellent agreement between numerical and analytical results, confirming the validity of the microcanonical method in the considered limit. In addition, since numerical results were obtained with the spatial dispersion taken into account, the comparison shows that the model with dispersionless phonons produces reliable results for LE even not very far away from the spectrum boundaries.

5. The solution in the vicinity of the spectrum boundary. Nonanalytical behavior.

The results obtained in the previous section are clearly not valid for frequencies close to the band boundaries ω_{il} and ω_{pu}, where $pf - \gamma = 0$ and the second term in the expansion (25) diverges. It is well known that perturbation expansions in disordered systems usually fail in the vicinity of boundaries of the initial spectrum of the system unperturbed by disorder.[25] The regions in the vicinity of these special frequencies ω_{il} and ω_{pu} require special consideration. Attempting to regularize our ϵ-expansion, we shall seek corrections to the zero order solution in the form

$$y = p + B\epsilon^{\alpha} \tag{41}$$

admitting a possibility of fractional values of α, and, hence, non-analytical behavior of the solution. We also introduce a new variable ζ which determines the proximity to either of two frequencies ω_{il} or ω_{pu}:

$$pf - \gamma = \zeta\epsilon^{\alpha'}. \tag{42}$$

Substituting these expressions into Eq. (22) and equating the lowest order terms we see that the equation can only be satisfied for $\alpha = \alpha' = 2/3$. In this case we find that the parameter B introduced in Eq. (41) obeys the equation

$$\frac{p(1-p)f}{2\sqrt{\zeta + Bf}} + B = 0. \tag{43}$$

The substitution of y given by Eq. (41) in the condition for the spectral boundaries presented by Eq. (24) allows

one to obtain an exact expression for the renormalized boundary

$$pf-\gamma=\left[3p^{2/3}(1-p)^{2/3}\left(\frac{-f}{2}\right)^{4/3}\right]\epsilon^{2/3}, \qquad (44)$$

that modifies Eq. (27). The shift is small by virtue of smallness of $\epsilon^{2/3}$. In the lowest order in ϵ, the new positions of the band edges for small p are

$$\widetilde{\omega}_{il}^2=\Omega_1^2-\frac{d^2\left(\Omega_1^2-\Omega_0^2\right)}{d^2-\left(\Omega_1^2-\Omega_0^2\right)}p\left[1+3\left(\frac{a}{4pl_0}\right)^{2/3}\right], \qquad (45)$$

$$\widetilde{\omega}_{pu}^2=\Omega_L^2+\frac{d^2\left(\Omega_1^2-\Omega_0^2\right)}{d^2-\left(\Omega_1^2-\Omega_0^2\right)}p\left[1-3\left(\frac{a}{16pl_0}\right)^{1/3}\right],$$

where we again encounter $a/(pl_0)$ as a true small parameter of the expansion. It is interesting to note the different character of non-analytical corrections to the positions of the boundary of the impurity band $\widetilde{\omega}_{il}^2$ and the bottom of the upper polariton branch $\widetilde{\omega}_{pu}^2$. They have fractional concentration dependence with the correction to $\widetilde{\omega}_{pu}^2$ being much stronger in the limit $a/(pl_0)\ll 1$.

Now let us consider the modification of LE and the integral DOS due to the nonanalyticity. Substituting Eq. (41) into Eq. (21) the complex LE can be written as

$$\widetilde{\lambda}=-\frac{p\left(1-p\right)f}{2B}\epsilon^{4/3}=\sqrt{\left(pf-\gamma\right)+Bf\epsilon^{2/3}}\cdot\epsilon. \qquad (46)$$

This expression explicitly demonstrates the crossover between analytical and nonanalytiacal behavior. When frequency ω lies far from the initial boundary $|pf-\gamma|\gg Bf\epsilon^{2/3}$, one recovers the term proportional to ϵ with the same coefficient as in Eq. (26), whereas in the opposite limit $|pf-\gamma|\ll Af\epsilon^{2/3}$, when we approach the boundary, the leading term gains fractional power and becomes $\propto\epsilon^{4/3}$.

At the vicinity of the renormalized spectral boundary, Eq. (45), DOS $\rho(\omega)\equiv 0$ to the left of $\widetilde{\omega}_{il}$ and for $\omega>\widetilde{\omega}_{il}$ it can be obtained as

$$\rho\left(\omega\right)=\frac{3}{\pi d}\left(\frac{\gamma}{l_0}\right)^{1/2}\frac{1}{\left(l_0p\right)^{1/2}}\frac{\omega}{\left(\omega^2-\widetilde{\omega}_{il}^2\right)^{1/2}}, \qquad (47)$$

where γ and l_0 are evaluated at $\omega=\Omega_1$, and we have neglected the renormalization of the boundary when calculating the coefficient in $\rho\left(\omega\right)$. In this approximation the frequency and concentration dependence of DOS does not change as compared to the one obtained from the non-renormalized expansion (33). It is interesting, however, that the renormalization brings about an additional numerical factor of 3 in Eq. (47), which is absent in the non-renormalized expression. This frequency dependence is typical for excitations with the quadratic dispersion law in the long-wave approximation. The main characteristics of this dispersion law is the effective mass m, which can be found from Eq. (47) as

$$m=\frac{9\gamma}{2pd^2l_0^2}=\frac{9\gamma^2}{2pc^2}\left(\frac{\omega_{il}}{d}\right)^2. \qquad (48)$$

It is interesting to compare this expression with the effective mass of the upper polariton branch of the pure system at the bottom of the band $2m_0=(\omega_L/dc)^2$. The two expressions have a similar structure if one introduces a "renormalized speed of light"

$$\tilde{c}=c\sqrt{p/9\gamma^2}. \qquad (49)$$

Though the introduced parameter $\tilde{c}$ does not have a direct meaning of the speed of the excitations, it shows again that the excitations in the impurity polariton band are considerably slower than their regular counterparts, with a similar dispersion law at the spectrum boundary as well as at the center of the band. Unlike, however, the center-of-band situation (39) the renormalized velocity at the edge is proportional to the square root of concentration.

LE in the vicinity of $\widetilde{\omega}_{il}$ is represented by different expressions for frequencies below and above $\widetilde{\omega}_{il}$ respectively

$$\lambda=\frac{1}{2l_0}\left(\frac{1}{4pl_0}\right)^{1/3}\left[1+\frac{12}{d}\frac{\left(\gamma l_0\right)^{1/2}}{\left(4l_0p\right)^{1/6}}\left(\widetilde{\omega}_{il}^2-\omega^2\right)^{1/2}\right], \qquad (50)$$

$$\lambda=\frac{1}{2l_0}\left(\frac{1}{4pl_0}\right)^{1/3}\left[1-\frac{12}{d^2}\frac{\gamma l_0}{\left(4l_0p\right)^{1/3}}\left(\omega^2-\widetilde{\omega}_{il}^2\right)\right],$$

reflecting a discontinuity of its frequency derivative at the spectrum boundary. LE itself is, of course, continuous at $\widetilde{\omega}_{il}$, giving rise to the localization length $l=2l_0\left(4pl_0\right)^{1/3}$ at the edge of the band. It is interesting to compare this expression with the localization length at the center of the impurity band, Eq. (40). They both grow with the concentration but the latter one is much smaller and demonstrates slower fractional concentration dependence.

At the upper impurity band edge Ω_1 integral DOS, $N(\omega)$, diverges causing much stronger singularity in the differential DOS than at the lower boundary ω_{il}

$$\rho\left(\omega\right)=\frac{d\omega p^{1/2}}{\pi c\left(\Omega_1^2-\omega^2\right)^{3/2}}, \qquad (51)$$

which is typical for DOS in the vicinity of resonance frequencies. Comparing this expression with a similar formula for a pure chain, one can again interpret this result as a renormalization of the velocity parameter c by the concentration of impurities, which is different from that presented by Eq. (49) by a numerical coefficient only.

The last spectrum boundary is the bottom of the upper polariton branch Ω_L. The spectrum in the vicinity of this frequency exists in the absence of the impurities, which are responsible for two effects in this region. First they move the boundary from Ω_L to higher frequencies [Eq. (45)], and second, they increase the effective mass

of the upper polariton branch, such that the differential DOS in the frequency region above $\widetilde{\omega}_{up}^2$ becomes

$$\rho(\omega) = \frac{1}{\pi dc} \frac{\omega}{\left(\omega^2 - \widetilde{\omega}_{up}^2(p)\right)^{1/2}} \times \left\{ 1 + \frac{p}{2} \left[\frac{d^2\left(\Omega_1^2 - \Omega_0^2\right)}{d^2 - \left(\Omega_1^2 - \Omega_0^2\right)} \right]^2 \right\}. \quad (52)$$

This expression can also be interpreted as a renormalization of the speed of light c.

IV. CONCLUSION

In the paper we have presented a detailed study of an impurity induced band of excitations, which arise in the gap between lower and upper polariton branches of a linear chain with dipole active atoms. We have also studied impurity-induced effects on properties of the regular polariton branches. The method of microcanonical ensemble in conjunction with the expansion in the parameter $l_{def}/l_0 \ll 1$, where l_{def} is the average distance between the impurities and l_0 is the localization radius of a single local polariton state, produces a clear physical description of the excitations, and shows excellent agreement with the results of numerical simulations. In the zero order of this expansion, we recover DOS and the dispersion law of excitations in the system with uniform continuously distributed impurities. Corrections to this solution describe effects due to local fluctuations in the positions of impurities such as a finite localization length of the excitations, a renormalization of the spectral boundaries and the effective mass of the excitations. The parameter l_{def}/l_0, therefore can be considered as a measure of disorder in the system.

The main result of the calculations is the demonstration of the existence of the polariton band formed by impurities without inner optical activity. Justification for naming these excitations as polaritons lies in the fact that they carry an electromagnetic field coupled with mechanical excitations of the chain. The dispersion law of the excitations at the lower frequency spectral boundary resembles that of the upper regular polariton band, but with a significantly (by a factor of $p^{1/2} \ll 1$) reduced effective mass. At the higher frequency edge of the band, the wave number diverges in a manner similar to the regular lower polariton branch with a velocity parameter again reduced by the same factor. The group velocity of the excitations near the center of the band, as well as is the localization length, is proportional to p. The latter, however, demonstrates a parabolic frequency dependence with the curvature of the parabola falling off with increase of the concentration as $1/p^2$. Excitations considered in this paper are drastically different from impurity-induced polaritons studied in Ref. 17. The authors of the latter paper considered excitations of an ordered chain of two-level atoms embedded in a polar 1-d crystal. Most significantly, the effective mass of polaritons of Ref. 17 is negative at the long-wave boundary of the spectrum while our excitations have a positive effective mass in this region; concentration dependencies of the effective mass and the band width also differ significantly.

The regular expansion in powers of the parameter l_{def}/l_0 produces diverging expressions at the boundaries of the zero order spectrum. Allowing for fractional powers in the expansion, we obtained a finite regularized expression for the density of states and the localization length at the boundaries. It is interesting to note that renormalized DOS at the lower boundary of the impurity band differs from its initial form only by a numerical factor of 3, while the position of the boundary is shifted toward lower frequencies.

Experimental significance of the considered excitations is affected by two factors: absorption due to different kind of anharmonic processes, and the one-dimensional nature of the considered model. It is generally accepted (see for instance Ref. 8) that one-dimensional models give a fair description of tunneling in the limit of small concentrations ($l_{def}/l_0 \gg 1$). We deal with the opposite limit; however, our zero order results could describe the dispersion law of excitations in the real three dimensional medium propagating in one specified direction (for example, the direction with the highest symmetry). Disorder in this case would lead, of course, to scattering and deviation from one-dimensional geometry, but effects due to disorder are much weaker in three dimensions, and would not probably inhibit an observation of a defect induced transparency in the frequency region of a polariton gap.

One can give a simple estimate for the role of absorption comparing the absorption coefficient with the width of the impurity induced band. If the latter is greater the band would manifest itself in transmission (or reflection) experiments. Using Eq. (31) one can obtain the following estimate for the admissible absorption coefficient α:

$$\alpha \ll \frac{d^2(\Omega_1^2 - \Omega_0^2)p}{\Omega_1\left(\Omega_L^2 - \Omega_1^2\right)}$$

if the defect frequency Ω_1 is not very close to the upper boundary of the gap Ω_L or

$$\alpha \ll \frac{d^2}{\Omega_L}\sqrt{p}$$

in the opposite case. The latter situation is much more favorable because of the square root concentration dependence. For example, for frequencies of the order of 1000 cm^{-1} and volume concentration of 0.1%, which correspond to linear concentration entering our formulas $p \sim 10\%$, one has from the last expression $\alpha \ll 300$ cm^{-1}, while the typical value of absorption for, e.g., alkali halides is ~ 100 cm^{-1}. This estimate shows that an observation of the transmittance through polariton gaps due to impurity polaritons is feasible.

V. ACKNOWLEDGMENT

We are pleased to acknowledge valuable remarks of A.J. Sievers. We wish to thank S. Schwarz for reading and commenting on the manuscript. This work was supported by the NSF under grant No. DMR-9632789 and by a CUNY collaborative grant.

---

[1] S. John, Phys. Rev. Lett. **53**, 2169 (1984).
[2] D.S. Wiersma, P. Bartolini, A.Lagendijk, and R. Righini, Nature **390**, 671 (1997).
[3] E. Yablonovitch, Phys. Rev. Lett. **58**, 2059 (1987).
[4] J.D. Joannopoulos, R.D. Meade, and J.N. Winn., *Photonic Crystals: Molding the Flow of Light* (Princeton University Press) 1995.
[5] S. John, Phys. Rev. Lett. **58**, 2486 (1987).
[6] I.M. Lifshitz, Nuovo Cim. (Suppl. A1) **3**, 591 (1956).
[7] I.M. Lifshitz and A.M. Kosevich, in: *Lattice Dynamics* (Benjamin, New York, 1969), p. 53.
[8] I.M.Lifshitz and Kirpichnikov, Sov. Phys. JETP **50**, p. 499 (1979).
[9] A.A. Maradudin, in: *Lattice Dynamics* (Benjamin, New York, 1969), p. 1
[10] Maradudin, E.W. Montroll, G.H. Weiss, and I.P. Ipatova *Theory of Lattice Dynamics in the Harmonic Approximation*, 2nd edition (Academic Press, New York, 1971).
[11] B.I. Schklovskii and A.L. Efros, *Electron Properties of Doped Semiconductors* (Springer, New York, 1984).
[12] E. Yablonovitch, Phys. Rev. Lett., **58**, 2059 (1987); S. John, T. Quang, Phys. Rev. A, **50**, 1764 (1994).
[13] E. Yablonovitch, T.J. Gmitter, R.D. Meade, A.M. Rappe, K.D. Brommer, and J.D. Joannopoulos. Phys. Rev. Lett. **67** 3380 (1991).
[14] R.D. Meade, K.D. Brommer, A.M. Rappe, and J.D. Joannopoulos, Phys. Rev. B **44** 13772 (1991).
[15] V.I. Rupasov and M. Singh, Phys. Rev. A, **54**, 3614 (1996); Phys. Rev. A **56**, 898 (1997).
[16] S. John, J. Wang, Phys. Rev. Lett., **64**, 2418 (1990); Phys. Rev. B, **43**, 12772 (1991).
[17] M. R. Singh and W. Lau, phys. stat. sol. (b) **203**, 401 (1997).
[18] L.I. Deych and A.A. Lisyansky, Bull. Amer. Phys. Soc. **42**, 203 (1997); Phys. Lett. A, **240**, 329 (1998).
[19] V.S. Podolsky, L.I. Deych, and A.A. Lisyansky, Phys. Rev. B, **57**, 5168 (1998).
[20] L.I. Deych and A.A. Lisyansky, Phys. Lett. A, **243**, 156 (1998).
[21] L.I. Deych, A. Yamilov and A.A. Lisyansky, Europhys. Lett., **46**, 534 (1999).
[22] L.I. Deych, A. Yamilov and A.A. Lisyansky, Phys. Rev. B, **59**, 11339 (1999).
[23] J. M. Deutsch and G. Paladin, Phys. Rev. Lett. **62**, 695(1989).
[24] D.J. Thouless, J.Phys.C, **5**, 77 (1972).
[25] I.M. Lifshitz, S.A. Gredeskul, L. A. Pastur, *Introduction to the theory of disordered systems.* (Wiley, New York, 1988).

FIG. 1. LE for a chain with a defect concentration of 10 % (solid line) in comparison to a pure system (dashed line).

FIG. 2. Dependences of LE (solid line) and DOS (dashed line) on concentration for a frequency in the interval $\Omega_0 < \omega < \Omega_1$.

FIG. 3. Comparison of LE calculated with (dashed line) and without (solid line) spatial dispersion in the vicinity of Ω_1. The concentration of defects for both curves is 1 %.

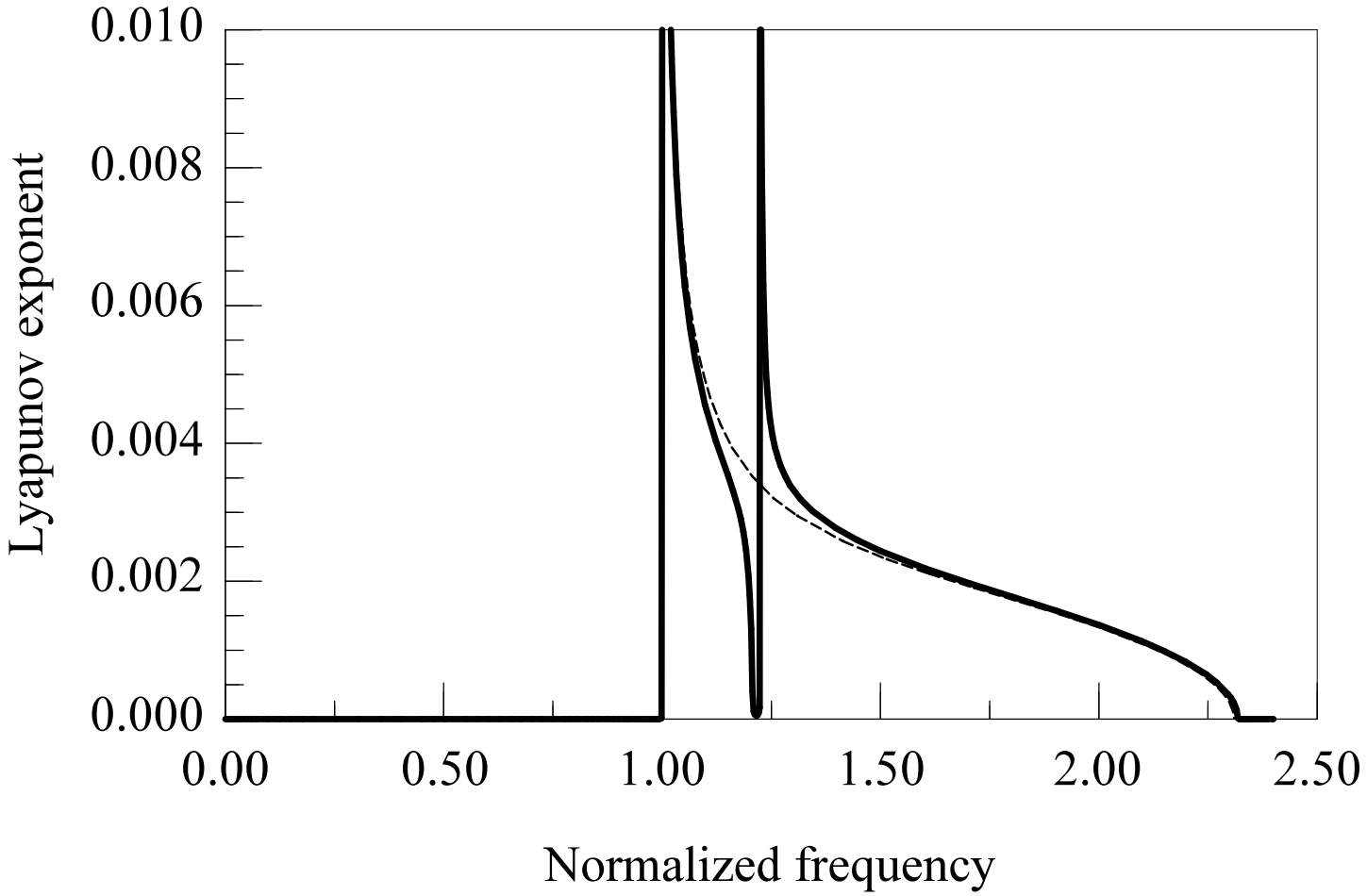
0.010
0.008
0.006
0.004
0.002
0.000
Lyapunov exponent
0.00
0.50
1.00
1.50
2.00
2.50
Normalized frequency

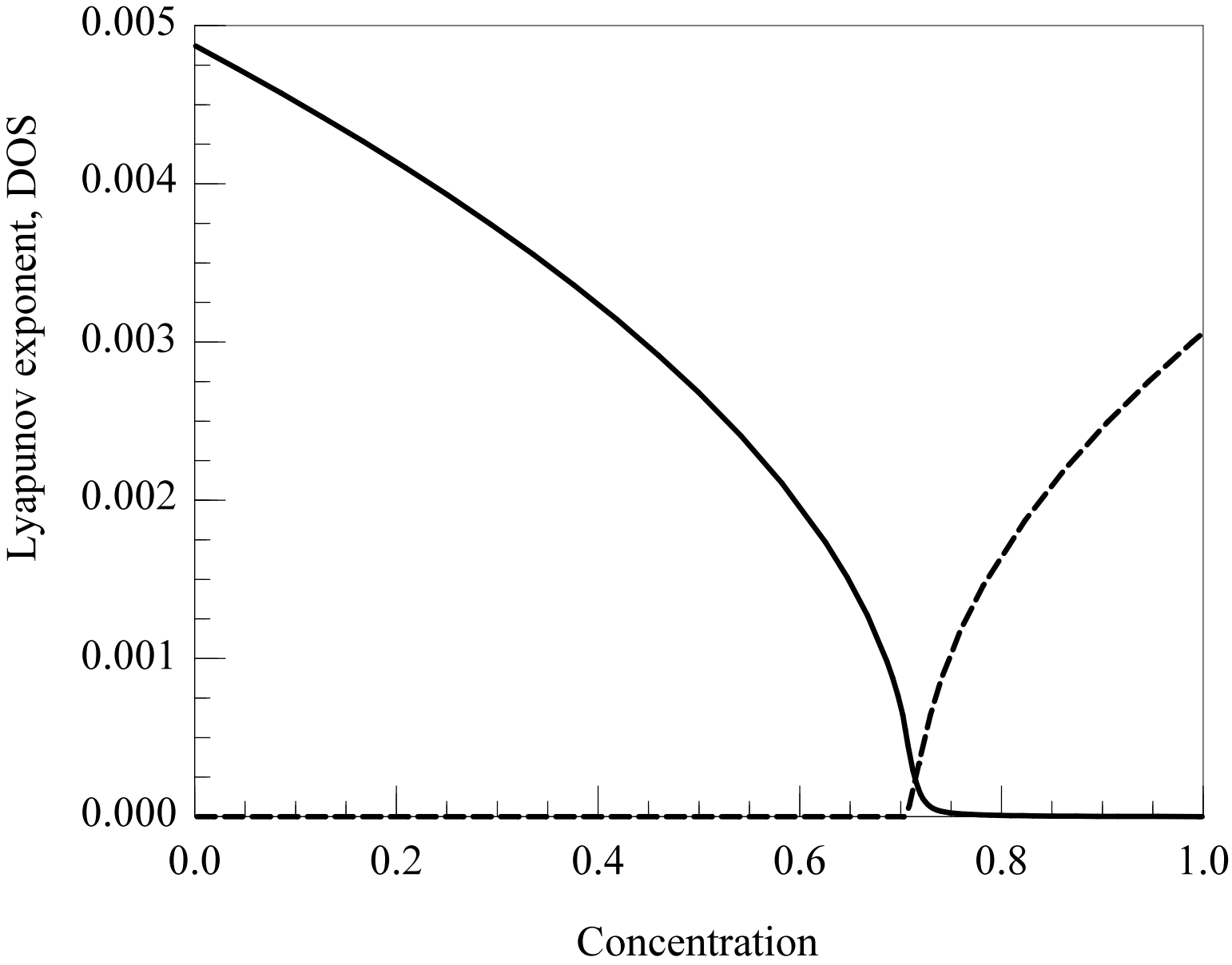
0.005
0.004
0.003
0.002
0.001
0.000
Lyapunov exponent, DOS
0.0
0.2
0.4
0.6
0.8
1.0
Concentration

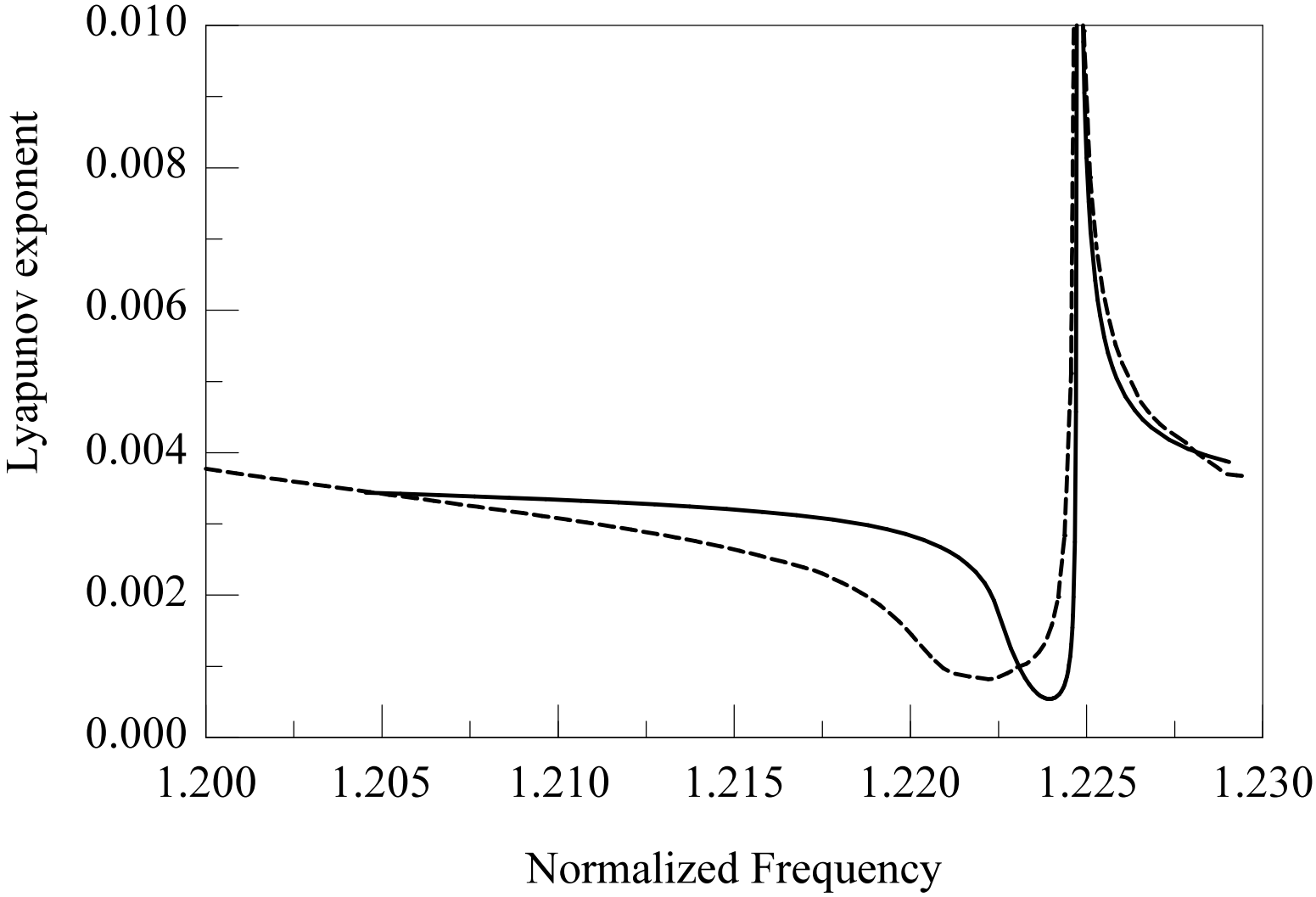
0.010
0.008
0.006
0.004
0.002
0.000
Lyapunov exponent
1.200
1.205
1.210
1.215
1.220
1.225
1.230
Normalized Frequency